For submission to ***Dalton Trans*** (40th Birthday Issue)

Structure-Activity Relationships for Organometallic Osmium Arene Phenylazopyridine Complexes with Potent Anticancer Activity

Ying Fu, Abraha Habtemariam, Aida M.B.H. Basri, Darren Braddick, Guy J. Clarkson and Peter J. Sadler*

Department of Chemistry, University of Warwick, Gibbet Hill Road, Coventry, CV4 7AL, U.K.

Abbreviations: NAC, N-acetyl-L-cysteine; bpy, 2,2'-bipyridine; L-BSO, L-buthionine-[S,R]-sulfoximine; 2-Br-Azpy, 4-bromo-2-(phenylazo)pyridine; 2-I-Azpy, 4-iodido-2-(phenylazo)pyridine; 1-CF_3-4-Cl-Azpy, 2-chloro-5-trifluoromethyl-2-(phenylazo)pyridine; 1-Cl-Azpy, 5-chloro-2-(phenylazo)pyridine; 2-F-Azpy, 4-fluoro-2-(phenylazo)pyridine; 2-Cl-Azpy, 4-chloro-2-(phenylazo)pyridine; 4-iodo-2-(phenylazo)pyridine; 3-Cl-Azpy, 3-chloro-2-(phenylazo)pyridine; Abpy, 2,2′-azobispyridine;OH-Azpy-NO_2, 5-hydroxy-2-(4-nitrophenylazo)pyridine. ROS, reactive oxygen species.

Electronic supplementary information (ESI) available: Abbreviations List, Synthesis and Characterizations of compounds 1-32, Tables S1 and S2 and Figure S1. X-ray crystallographic CIF files for complexes **18**, **16**, **14**, **13**, **19**, **10**, **7**, **24**, **20**, and **26** have been deposited in the CCDC with reference numbers 821519 – 821528, respectively.

*To whom correspondence should be addressed. Phone: (+44) 024 7652 3818. Fax: (+44) 024 7652 3819; E-mail: P.J.Sadler@warwick.ac.uk.

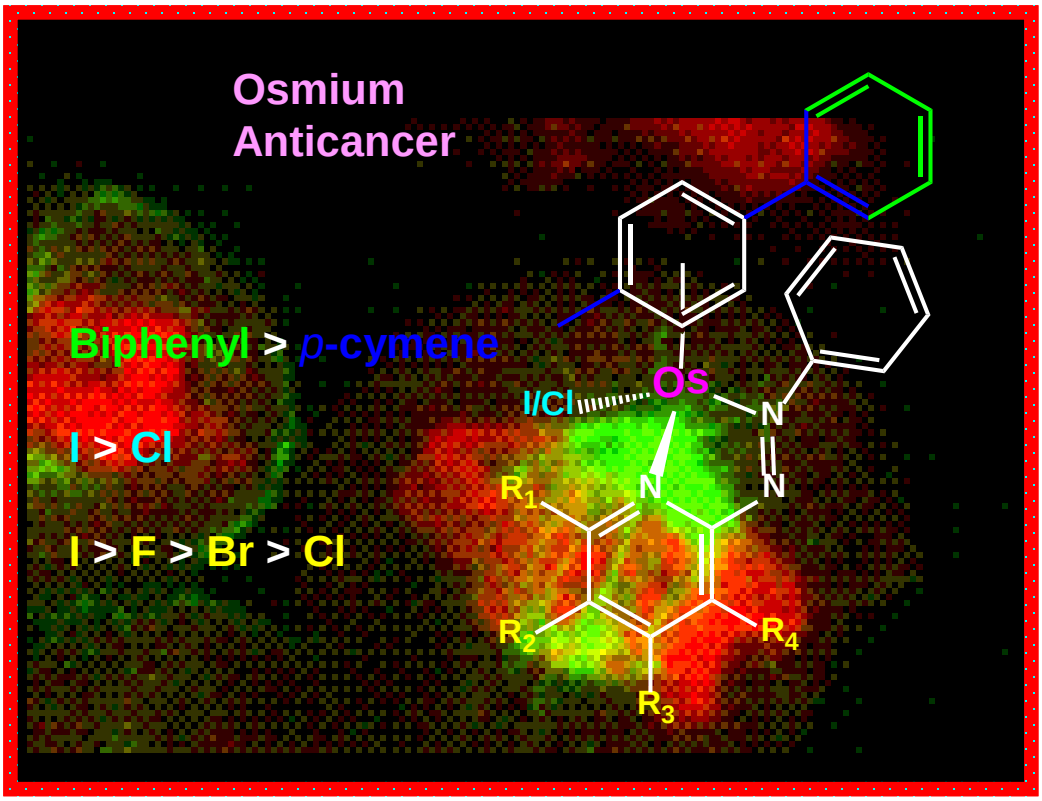
Osmium
Anticancer
Biphenyl > p-cymene
I > Cl
I > F > Br > Cl
I/Cl
Os
N
N
N
R1
R2
R3
R4

Abstract

We report the synthesis and characterisation of 32 half sandwich phenylazopyridine Os^{II} arene complexes $[Os(\eta^6\text{-arene})(\text{phenylazopyridine})X]^+$ in which X is chloride or iodide, the arene is *p*-cymene or biphenyl and the pyridine ring contains a variety of substituents (F, Cl, Br, I, CF_3, OH or NO_2). Ten X-ray crystal structures have been determined. Cytotoxicity towards A2780 human ovarian cancer cells ranges from high potency at nanomolar concentrations to inactivity. In general the introduction of an electron-withdrawing group (e.g. F, Cl, Br or I) at specific positions on the pyridine ring significantly increases cytotoxic activity and aqueous solubility. Changing the arene from *p*-cymene to biphenyl and the monodentate ligand X from chloride to iodide also increases the activity significantly. Activation by hydrolysis and DNA binding appears not to be the major mechanism of action since both the highly active complex $[Os(\eta^6\text{-bip})(2\text{-F-azpy})I]PF_6$ (**9**) and the moderately active complex $[Os(\eta^6\text{-bip})(3\text{-Cl-azpy})I]PF_6$ (**23**) are very stable and inert towards aquation. Studies of octanol/water partition coefficients (log P) and subcellular distributions of osmium in A2780 human ovarian cancer cells suggested that cell uptake and targeting to cellular organelles play important roles in determining activity. Although complex **9** induced the production of reactive oxygen species (ROS) in A2780 cells, the ROS level did not appear to play a role in the mechanism of anticancer activity. This class of organometallic osmium complexes has new and unusual features worthy of further exploration for the design of novel anticancer drugs.

Introduction:

The 'from bench to clinic' story of cisplatin[1] has simulated the search for other transition metal anticancer complexes with improved features. In particular some group 8 organometallic complexes of iron, ruthenium and osmium show promising activity.[2, 3] For example, Jaouen et al. have designed ferricenium complexes which target hormone receptors in breast cancer cells,[4] certain Ru^{II} arene complexes are active *in vitro* and *in vivo*,[5-7],[8] and a few reports of anticancer active organometallic osmium complexes have recently appeared.[9-15]

Osmium complexes are often considered to be relatively inert (a common characteristic of low-spin d^6 metal ions and especially 3rd row transition metals).[16, 17] Organometallic Os^{II} and Ru^{II} arene complexes can adopt very similar three-dimensional structures. For example, for the kinase inhibitors designed by Meggers et al.[18], both osmium and ruthenium analogues are part of an inert scaffold that neatly fits into the active site of the enzyme and promotes specific outer-sphere contacts between groups on the ligands and the enzyme. There can also be intriguing differences between the chemical properties of organometallic Ru^{II} and Os^{II} arene complexes even though their three-dimensional structures are almost identical. For example, the hydrolysis rate of chlorido arene complexes of Os^{II} is often ca. 100x slower that for Ru^{II}, and the resulting aqua Os^{II} complexes are ca, 1.5 pK_a units more acidic.[17] Moreover, Ru^{II} and Os^{II} complexes can exhibit differences in their medicinal properties. For example, the osmium analogue of the ruthenium antimetastatic drug NAMI-A [trans-tetrachloro(1H-imidazole)(S-dimethylsulfoxide)ruthenate(III)] exhibits better *in vitro* anticancer activity.[19]

The only recognised clinical use of osmium appears to be for synovectomy in arthritic patients in Scandinavia.[20-22] This involves the local administration of osmium tetroxide (OsO_4), usually considered to be a highly toxic compound. The lack of reports of long term side effects suggest that osmium itself can be biocompatible,

although clearly this might be dependent on the exact nature of the compound administered. Osmium carbohydrate polymers (osmarins) have been also investigated as potential antiarthritic agents.[23]

Recently, non-organometallic osmium(VI) complexes were reported to show anticancer activity *in vivo*.[12] We have also reported that certain half-sandwich organometallic iodido osmium phenylazopyridine arene complexes exhibit potent *in vitro* and *in vivo* anticancer activity, higher activity than the clinical drug cisplatin to a panel of cancer cell lines *in vitro*.[24, 25] Similar to Ru^{II},[26] we have found that the introduction of the strong π-acceptor azopyridine as a ligand in organometallic Os^{II} complexes has a major effect on their chemical and biological properties.[12]

For Os^{II} arene picolinate complexes, log P values correlate with cellular uptake, which indicates that increased lipophilicity favours uptake by cancer cells, probably through a passive diffusion pathway, and results in an increase in anticancer activity.[27] However, increasing lipophilicity to improve anticancer activity can result in difficulties with clinical formulation and lower bioavailability[28]. Hence there is a need for rational design aimed at tuning lipophilicity while maintaining anticancer activity.

The goal of anticancer research programs is to identify novel, synthetically-feasible molecules that exhibit useful anticancer activity with minimal side-effects. One efficient approach is the study of bioisosterism, a term coined to describe the modification of biological activity by isosterism.[29-31] Here we report studies of a series of novel bioisosteres of Os^{II} arene complexes containing chelated phenylazopyridines with various substitutents on the pyridine ring. We show that cellular reactive oxygen species (ROS) accumulate but do not lead to the death of cancer cells, suggesting a mechanism different from that for related complexes with an unsubstituted pyridine ring and a substitutent on the phenyl ring. In addition, it is found that down-regulation of the cellular GSH level results in lowering of anticancer activity, a property which

has been found only for the anticancer drug taxol, which binds to tubulin in a GSH-dependent manner.[32]

Results

Previously we reported the synthesis and cancer cell cytotoxicity of twelve osmium(II) phenylazopyridine complexes containing various substituents on the phenyl ring.[24] The least active compounds in this class contained unsubstituted phenyl rings.[24] In the present work, we have investigated whether the latter complexes can be activated by introducing substituents (R) into the pyridine ring in the class [Os(η^6-*p*-cym)(R-Azpy)X]PF_6. We have also investigated the effect of changing the arene ligand (from *p*-cymene to biphenyl) and the monodentate ligand (X) from Cl to I. The exploration of such a family of bioisosteres may allow optimisation of properties and allow discovery of candidates ('hits') suitable for preclinical development.

In total, 32 novel complexes were synthesized (Chart 1) in good yields, with PF_6^- as the counter anion, and characterized by elemental analysis, ESI-MS and NMR spectroscopy. For ten complexes, X-ray crystal structures were determined.

X-ray Crystal structures. Eighteen novel iodido osmium complexes were synthesized and the structures of [Os(η^6-bip)(2-Cl-Azpy)I]PF_6 (**13**), [Os(η^6-*p*-cym)(2-Cl-Azpy)I]PF_6 (**14**), [Os(η^6-*p*-cym)(2-Br-Azpy)I]PF_6 (**18**) and [Os(η^6-*p*-cym)(3-Cl-Azpy)I]PF_6 (**24**) were determined by X-ray crystallography. For comparison, fourteen chlorido analogues were synthesized and the structures of the complexes [Os(η^6-bip)(1-Cl-Azpy)Cl]PF_6 (**7**), [Os(η^6-bip)(2-F-Azpy)Cl]PF_6 (**10**), [Os(η^6-*p*-cym)(2-Cl-Azpy)Cl]PF_6 **(16)**, [Os(η^6-bip)(2-Br-Azpy)Cl]PF_6 (**19**), [Os(η^6-*p*-cym)(2-Br-Azpy)Cl]PF_6 (**20**) and [Os(η^6-*p*-cym)(3-Cl-Azpy)Cl]PF_6 (**26**) were also determined by X-ray crystallography (Fig 1, Tables S1 and S2). All adopt the familiar half-sandwich 'piano-stool' geometry.

Stability and Hydrolysis. We investigated the hydrolysis (aquation) of these azopyridine complexes since this is a potential mechanism for activation of halido osmium arene complexes in their interactions with biological targets such as DNA.[33] The aqueous behaviour of the highly active complex **9** [Os(η^6-bip)(2-F-Azpy)I]PF_6 and moderately active complex **23** [Os(η^6-bip)(3-Cl-Azpy)I]PF_6 was studied at 310 K. The UV-Vis spectra, showed no change after 24 h, (Fig S1) indicating that complexes **9** and **23** remained stable and did not hydrolyze over that period, similar to the highly active azopyridine complexes containing unsubstituted pyridine rings that we reported previously.[24]

Structure-Activity Relationships Based on Bioisosteres. We investigated the effect of F, Cl, Br, I and CF_3 substituents in the R_1-R_4 positions of the pyridine ring of the phenylazopyridine chelating ligand (Chart 1) on the cytotoxicity of the complexes towards human ovarian A2780 cancer cells (Table 1A).

Their potency covers a wide range of concentrations, from very high potency with an IC_{50} of 220 nM for complex **21**, [Os(η^6-bip)(2-I-Azpy)I]PF_6, to >100 μM and inactivity for complexes **10**, **25**, **26** and **30**, Table 1. The following trends are observed:

(1) Complexes containing iodide as the monodentate ligand have a higher activity compared to the chlorido complexes (Table 1B).

(2) Biphenyl complexes are, in general, 10 times more active than *p*-cymene complexes (Table 1C).

(3) The effect of chloride as an electron-withdrawing group on the pyridine ring depends on its position. Changing the electron-withdrawing group at the R_2 position leads to increases in activity in the order Cl < Br ≤ F < I.

(4) Within the most active series, which contain biphenyl as the arene and iodide as the monodentate ligand, anticancer activity decreases with pyridine ring substitution position in the order $R_2 > R_1 > R_3$, with [Os(η^6-bip)(2-Cl-Azpy)I]PF_6 (**13**) being the most active, (IC_{50}= 1 μM) (Fig. 2A).

(5) Changing the phenyl ring in the phenylazopyridine chelating ligand to pyridine, does not improve the anticancer activity (Fig. 2B). Also it is notable that that the osmium(II) chlorido and iodido complexes with 5-hydroxy-2-(4-nitrophenylazo)pyridine as the chelating ligand showed similar activity (Table 1A).

Partition Coefficients (Log P). Octanol/water partition coefficients (log P values) provide a measure of the lipophilicity of compounds and are often a useful indication of the likely extent of drug uptake by cells.[34] We determined log P values for four iodido complexes **9** (2-F), **13** (2-Cl), **17** (2-Br), and **23** (3-Cl), and two chlorido complexes **19** (2-Br), and **25** (3-Cl), all biphenyl arene complexes, using the "shake tube method". The log P values for these complexes (Table S3) decrease along the series: complex **19** (monodentate ligand Cl/substituent 2-Br) > **17** (I/2-Br) > **13** (I/2-Cl) > **23** (I/3-Cl) > **9** (I/2-F)> **25** (Cl/3-Cl) (Fig. 3), ranging from 0.1330 (partitioning preferentially into octanol) to -1.446 (partitioning preferentially into water).

Cellular uptake and distribution in A2780 cells. Time-dependent cellular uptake studies of the biphenyl/iodido complexes **9** [Os(bip)(2-F-Azpy)I]PF_6 and **23** [Os(bip)(3-Cl-Azpy)I]PF_6 showed that the accumulation of **9** is much higher than that of **23** after 24 h (Fig. 4A) The distribution of Os in A2780 cells was investigated after incubation with 4 μM complex **9** or **23.** The cytosol, membrane-plus-particulate fraction, nucleus and cytoskeleton fractions were separated and their Os contents determined by ICP-MS (Fig. 4B). Complex **9** gave rise an uptake of osmium into the cytosol, membrane plus particulate fraction and nucleus ca. 23 times higher than for **23** (Fig. 4B, Table. S4). It is interesting that for **23** there is a very high percentage of osmium in the cytoskeleton, up to 43 % of the total cellular Os (Fig S2).

Detection of ROS in A2780 Cancer Cells. To detect changes in general oxidative stress,[35] we determined the level of reactive oxygen species (ROS, including O_2^-, $OH^{\cdot}$, H_2O_2) in A2780 cells using the probe 2′,7′-dichlorodihydrofluorescein-diacetate (DCFH-DA). When taken up by live cells, DCFH-DA hydrolyzes to 2′,7′-

dichlorodihydrofluorescein (DCFH), which in turn is oxidized to 2′,7′-dichlorofluorescein (DCF) in the presence of ROS and detected by its intense fluorescence.[36, 37] We investigated the change in ROS level induced by **9,** [Os(η^6-bip)(2-F-Azpy)I]PF_6, one of the most active compounds. The relative increase in DCF fluorescence was detected over time after exposure to **9** alone (1 μM), **9** (1 μM) with L-buthionine sulfoximine (L-BSO, 50 μM, an inhibitor of glutamylcysteine synthetase)[38], and, for comparison, H_2O_2 (50 μM). For **9**, an increase in intracellular ROS level was observed, but it was lower than that observed for H_2O_2 (50 μM) after 4 h incubation.

Exposure of A2780 cells to **9** (1 μM) in the presence of the antioxidant thiol N-acetyl-L-cysteine (NAC, 50 μM) [39] gave no increase in ROS level compared to the control. However, for **9** (1 μM) with L-BSO (50 μM), the increase in ROS level was even higher than that for H_2O_2 (50 μM). (Fig 5A) The increase of fluorescence over time after exposure of A2780 cells preloaded with DCFH-DA to 1 μM of **9**, indicates that **9** causes a build-up of ROS inside A2780 cancer cells.

Relationship of Cytotoxicity to ROS. In order to further investigate the possible involvement of ROS in the cytotoxicity of the phenylazopyridine osmium arene complexes studied here, we also investigated the combined effects of either complex **9** or **17** with the reductant NAC which can deplete ROS or with L-BSO which depletes glutathione levels and can lead to an increase in levels of ROS in cells.

The cytotoxicity assays showed that complex **9** (1 μM) in combination with the reductant (antioxidant) NAC (50 μM) did not increase the survival of A2780 cells compared to those treated with **9** alone for 24 h (Fig 5B). This suggests that ROS are not implicated in cell death induced by complex **9**. In contrast, combination treatment with the oxidant L-BSO, which resulted in an increase in the ROS level, blocked the anticancer activity.

The effect of combination treatment with the reductant (antioxidant) NAC (50 μM) on IC_{50} values for complex **9** was investigated for both A2780 (ovarian) and A549 (lung) human cancer cell lines (Table 2). A2780 cells were treated with various concentrations of **9** or **17** together with NAC (50 μM). Combination treatment with NAC decreased the cytotoxicity of both **9** and **17**, slightly. However, combination treatment with L-BSO raised the IC_{50} values for **9** and **17** more than 10 times for A2780 cells. For the A549 cell line, the IC_{50} value of **9** was raised from 1.8 μM to more than 100 μM, and for **17** the IC_{50} values increased more than 70-fold (Table 2). Intriguingly, these data resemble those reported for the effects of combination treatment on the organic drug Paclitaxel (Taxol) which is in clinical use for the treatment of ovarian, breast and non-small cell lung cancer. Taxol is known to target tubulin in microtubules.[32]

Discussion

In our previous studies we found that replacement of the N,N-chelating ligand ethylenediamine by phenylazopyridine in $[Ru(\eta^6\text{-arene})(N,N)X]^+$ complexes introduced some dramatic changes in their chemical and biological properties.[26] Phenylazopyridine ligands are not only σ-donors (like en), but also strong π-acceptors. The chlorido phenylazopyridine complexes $[Ru\ (\eta^6\text{-arene})\ (Azpy)Cl]^+$ (arene - p-cymene (*p*-cym), tetrahydronaphthalene (thn), benzene (bz), or biphenyl (bip) readily underwent slow decomposition via hydrolysis and/or arene loss. They were inactive (non-cytotoxic) towards cancer cells but activated by the introduction of electron-donating substituents into the phenyl ring, e.g. OH and NMe_2. The π-acceptor property of the phenylazopyridine ligand results in highly acidic aqua complexes. For example, the pK_a of the coordinated water in $[(\eta^6\text{-}p\text{-cym})Ru(Azpy\text{-}NMe_2)OH_2]^{2+}$ is 4.60.[40] Most dramatic was the effect of changing the monodentate leaving group from chloride to iodide which conferred on the complexes remarkable inertness towards ligand substitution.[26] Moreover these iodido complexes with substituents on the phenyl ring were highly cytotoxic to A2780 human ovarian and A549 human lung

cancer cell lines with IC_{50} values of 2 - 6 μM. The mechanism of cytotoxicity appeared to involve ligand-based redox reactions.[26]

These findings for Ru^{II} complexes appear to be mirrored to some extent for Os^{II} complexes. The chlorido Os^{II} phenylazopyridine complex [Os(η^6-*p*-cym)(Azpy)Cl]PF_6 is inactive towards A2780 human ovarian cancer cells but active with electron-donor NMe_2 or OH substituents on the phenyl ring. [24] The iodido complexes are more active and complexes with moderate activity e.g. [Os(η^6-*p*-cym)(Azpy)I]PF_6 (IC_{50} = 10.3 μM in A2780 cell line) become potently cytotoxic at nanomolar concentrations towards a panel of human cancer cell lines when substituents are introduced into the phenyl ring, e.g. IC_{50} = 140 nM for [Os(η^6-bip)(Azpy-NMe_2)I]PF_6 towards A2780 ovarian cancer cells.[24]

The aim of the current work was to investigate the effects on anticancer activity of introducing substituents into the pyridine ring especially when the phenyl ring is left unsubstituted. We synthesised and characterized 32 novel organometallic osmium phenylazopyridine complexes (Chart 1). All the osmium complexes adopted the familiar piano-stool geometry in the crystalline state, with bond lengths and angles within the expected ranges.[24] Selected bond lengths and angles for these structures are listed in the supporting information (Table S2). For the iodido osmium complexes, the Os-C (arene) bond lengths are in the range of 2.172-2.284 Å, and the Os-I bond lengths from 2.7002-2.7063 Å (Table S2). For the chlorido osmium complexes, the Os-C (arene) bond lengths are in the range of 2.173-2.286 Å, and Os-Cl bond lengths are 2.3727-2.3954 Å (Table S2). A relatively longer bond length for Os(1)-N(1)(pyridine) compared to Os(1)-N(8)(azo) was observed in all the 10 crystal structures. This can be attributed to the back-bonding competition for the osmium $5d^6$ electron density by the phenylazopyridine and arene -acceptor ligands. A similar trend was also observed for ruthenium arene phenylazopyridine complexes.[40] The longest Os(1)-N(1) bond length is 2.124(9) Å in [Os(η^6-bip)(1-Cl-Azpy)Cl]PF_6 (**7**), the structure determined for a complex with an ortho pyridine substituent (Cl), Table S2.

Three of the structures show π-π stacking. [Os(η^6-bip)(2-F-Azpy)Cl]PF_6 (**10**) exhibits intramolecular π-π stacking between the phenyl ring of the biphenyl arene ligand and the phenyl ring of the phenylazofluoropyridine ligand. There is also intermolecular π-π stacking involving the same groups, but between symmetry-related molecules. For [Os(η^6-*p*-cym)(3-Cl-Azpy)I]PF_6 (**24**), there is π-π stacking between the *p*-cymene and a phenyl ring in a symmetry-related molecule. There is an intermolecular π-π stacking interaction between 2-Cl-Azpy ligands that lie in a head-to-tail dimer fashion related by an inversion centre in [Os(η^6-*p*-cym)(2-Cl-Azpy)I]PF_6 (**14**). The distances between the planes of the stacked rings (ca. 3.3 Å) are within the normal range for such interactions.[41]

Remarkably electron-withdrawing substituents on the pyridine ring can give rise to highly potent complexes with IC_{50} values in the nano-molar range (Table 1A and Fig. 2). The structure-activity relationships show that potency is higher for biphenyl versus *p*-cymene as the arene (Table 1C), and for iodide compared to chloride as the monodenate ligand (Table 1B). Biphenyl is a stronger π-acceptor than *p*-cymene (back-donation of electron density from Ru^{II}) whereas *p*-cym is the stronger electron donor. When Ru^{II} arene complexes bind to DNA, the uncoordinated phenyl ring of bip can intercalate between DNA bases whereas DNA distortions caused by p-cymene are steric in origin.[42] The arene can also have a major effect on interactions with protein targets, as demonstrated for interactions between serum albumin and biphenyl and *p*-cymene Ru^{II} complexes.[43]

The inertness of the most active complexes to hydrolysis suggests direct binding to DNA is not the major mechanism of action and that a novel target for these metal arene complexes is involved. This was also the conclusion from our recent work on Os^{II} phenylazopyridine complexes containing unsubstituted pyridine and substitutions of the phenyl ring.

Reactive oxygen species (ROS) play important roles in regulating cell proliferation, death, and senescence, they can also play significant roles in the mechanism of action of anticancer agents.[44] We suggested previously that the cytotoxicity mechanism for osmium arene phenylazopyridine iodido complexes containing unsubstituted ($R_1 - R_4$ = H) pyridine rings and their ruthenium analogues is related to ROS generation.[26] However, the complexes investigated in the current work containing substituted pyridine rings do not appear to share a mechanism dependent to the formation of ROS. Down-regulation of ROS by increasing intracellular GSH, does not block the anticancer activity of **9** and **17**. It is also known that cisplatin resistance is partly related to an increase of GSH levels,[45] and the data for complexes **9** and **17** suggest that they have potential for the treatment of cisplatin-resistant tumours.[46]

The mechanism of action of complexes **9** and **17** is GSH-dependent. L-buthionine sulfoximine (L-BSO) depletes intracellular glutathione levels by inhibiting the enzyme glutamylcysteine synthetase. L-BSO is on clinical trial for combination treatment with Melphalan,[47] and increases the cytotoxicity of a number of therapeutic agents, including cisplatin, especially towards resistant cancer cell lines.[48, 49] The only reported exception in which the L-BSO can block the cytotoxicity of a drug appears to be taxol.[32] Our report is apparently only the second in which a blocking of anticancer activity by L-BSO has been observed.

For the structure activity relationships, it is evident that when biphenyl is the arene and iodide is the monodentate ligand, the osmium complexes in this class show the highest anticancer activity towards A2780 cells, consistent with our previous work on phenylazopyridine complexes with unsubstituted pyridine rings.[24] In our previous work some chlorido complexes were found to be unstable in aqueous solution which resulted in low anticancer activity.[24, 40] Introducing biphenyl as the arene instead of *p*-cymene not only provides a potential DNA intercalator but also increases the

hydrophobicity for interaction with proteins which may contribute to the increased activity.[5, 50]

Consideration of the substituents on the pyridine ring shows that changing from chloride at R_3 to fluoride causes the cellular accumulation of osmium to increase dramatically and is accompanied by an improvement in anticancer activity. The difference in the extent of cellular accumulation within this family may contribute to the observed variations in anticancer activity, as may interactions with targets (which may be proteins) .[50]

To investigate whether there is a link between lipophilicity and anticancer activity for these complexes. The log P values were determined; they cover a broad range from -1.446 to 0.1330 (Table S3). These values can be compared to those for the less lipophilic clinical Pt^{II} drug cisplatin (log P = -2.36)[51] and to the Ru^{III} drug NAMI-A (log P = -0.25)[52] which is on clinical trials as an antimetastatic agent. The sequence of potency towards A2780 human ovarian cancer cells for the osmium phenylazopyridine complexes is: **17** > **9** > **13** > **23** > 1**9** > **25**, whereas lipophilicity decreases in the order **9** (monodentate ligand Cl/ pyridine substituent 2-Br) > **17** (I/2-Br) > **13** (I/2-Cl) > **23** (I/3-Cl) > **9** (I/2-F)> **25** (Cl/3-Cl). Hence there appears to be little correlation between lipophilicity (log P), and anticancer activity (Fig. 3 and Table. S3). The introduction of bioisosterism into the design has led to the discovery of compounds with different pharmaceutical properties, potential candidates for further pharmacokinetic studies.

The cell distribution studies showed a dramatic increase in accumulation of osmium in the membrane and particulate fraction of A2780 cells for **9** compared to **23**, and **9** is more than 50 times more active than **23**. Whether the critical target site is in the membrane and particulate fraction remains to be investigated further. However, to identify and determine the contribution of the individual binding sites is a complex task, for example, only ca. 1 % of Pt from intracellular cisplatin binds to its target,

DNA,[53,54] Further work is required to validate the target for this sub-family of osmium arene phenylazopyridine complexes.

Experimental section

Materials. $OsCl_3 \cdot 3H_2O$ and osmium Specpure Plasma Standard were purchased from Alfa-Aesar. Ethanol and methanol were dried over Mg/I_2 or anhydrous quality was used (Aldrich). All other reagents used were obtained from commercial suppliers and used as received. The preparation of the starting materials $[Os(\eta^6\text{-bip})Cl_2]_2$ and $[Os(\eta^6\text{-}p\text{-cym})Cl_2]_2$ have been previously reported.[55] The synthesis of the phenylazopyridine ligands has been previously described.[26] The A2780 human ovarian carcinoma cell line was purchased from European Collection of Animal Cell Cultures (Salisbury, UK), RPMI-1640 media and trypsin were purchased from Invitrogen, bovine serum from Biosera, penicillin, streptomycin, trichloroacetic acid (TCA) and sulforhodamine B (SRB) from Sigma-Aldrich, and tris[hydroxymethyl]aminomethane from Formedium.

Instrumentation and methods

NMR Spectroscopy. ^{1}H NMR spectra were acquired in 5 mm NMR tubes at 298K on either Bruker DPX-400, Bruker DRX-500 or Bruker AV II 700 spectrometers. ^{1}H NMR chemical shifts were referenced to acetone-d_6 (2.09 ppm). All data processing was carried out using MestReC or TOPSPIN version 2.0 (Bruker U.K. Ltd.).

Electrospray Ionisation Mass Spectrometry (ESI-MS). Spectra were obtained by preparing the samples in 50% CH_3CN and 50% H_2O (v/v) and infusing into the mass spectrometer (Varian 4000). The mass spectra were recorded with a scan range of m/z 500-1000 for positive ions.

Elemental Analysis. Elemental analysis (carbon, hydrogen, and nitrogen) was carried out through Warwick Analytical Service using an Exeter analytical elemental analyzer (CE440).

UV-Vis Spectroscopy. UV-Vis spectra were recorded on a Cary 50-Bio spectrophotometer using 1-cm path-length quartz cuvettes (0.5 mL) and a PTP1 Peltier temperature controller. Spectra were recorded at ca. 310 K in double distilled water from 800 to 200 nm. Further details are in the SI.

pH* Measurements. pH* (pH meter reading from D_2O solution without correction for effects of deuterium on glass electrode) values were measured at ambient temperature before the NMR spectra were recorded, using a Corning 240 pH meter equipped with a microcombination electrode calibrated with Aldrich buffer solutions at pH 4, 7 and 10.

X-ray Crystallography. X-ray diffraction data for [Os(η^6-bip)(1-Cl-Azpy)Cl]PF_6 (**7**) [Os(η^6-bip)(2-F-Azpy)Cl]PF_6 (**10**, [Os(η^6-bip)(2-Cl-Azpy)I]PF_6 (**13**), [Os(η^6-*p*-cym)(2-Cl-Azpy)I]PF_6 (**14**), [Os(η^6-*p*-cym)(2-Cl-Azpy)Cl]PF_6 (**16**), [Os(η^6-*p*-cym)(2-Br-Azpy)I]PF_6 (**18**), [Os(η^6-bip)(2-Br-Azpy)Cl]PF_6 (**19**), [Os(η^6-*p*-cym)(2-Br-Azpy)Cl]PF_6 (**20**), [Os(η^6-*p*-cym)(3-Cl-Azpy)I]PF_6 (**24**) and [Os(η^6-*p*-cym)(3-Cl-Azpy)Cl]PF_6 (**26**) were obtained on an Oxford Diffraction Gemini four-circle system with a Ruby CCD area detector using Mo Kα radiation.[56] Absorption corrections were applied using ABSPACK. The crystals were mounted in oil and held at 100(2) K with the Oxford Cryosystem Cryostream Cobra, except compound **7** for which data was collected at ambient temperature. The structures were solved by direct methods using SHELXS (TREF) with additional light atoms found by Fourier methods.[57] Refinement used SHELXL 97.[58] H atoms were placed at geometrically calculated positions and refined riding on their parent atoms. X-ray crystallographic CIF files for complexes **18**, **16**, **14**, **13**, **19**, **10**, **7**, **24**, **20**, and **26** have been deposited in the CCDC with reference numbers 821519 – 821528, respectively.

Cell Cultures. A549 non-small cell lung and A2780 ovarian human cell lines (ECACC, Salisbury, UK) were cultured in RPMI 1640 cell culture medium supplemented with 1 mM sodium pyruvate, 2 mM L-glutamine and 10% fetal bovine serum (all from Sigma).

Synthesis: Complexes **1**–**32** were prepared by the same general method: reaction of the appropriate phenylazopyridine derivative with the dimers; $[Os(\eta^6\text{-bip})Cl_2]_2$, $[Os(\eta^6\text{-bip})I_2]_2$, $[Os(\eta^6\text{-}p\text{-cym})Cl_2]_2$ or $[Os(\eta^6\text{-}p\text{-cym})I_2]_2$. The purities of all compounds (**1**-**32**) prepared were determined to be ≥95% by elemental analysis. Single crystals suitable for X-ray diffraction were obtained by crystallization from methanol solutions at 253 K. The details of the syntheses and characterizations are in the Supporting Information.

Methods

Determination of IC_{50} Values. The concentrations of the osmium complexes that inhibit 50% of the proliferation of human ovarian A2780 cancer cells were determined using the sulforhodamine B assay.[59] A2780 cells were seeded in 96-well plate (Falcon) at 5000 cells/well, after the incubation for 48 h. The complexes were solubilised in DMSO (Sigma) to provide 10 mM stock solutions. These were serially diluted by cell culture media to give concentrations four-fold greater than the final concentrations for the assay. The complexes diluted in cell culture media were added to the 96-well plate with cells in triplicate. The final DMSO concentration in each well was no more than 1% (v/v). The media containing the complexes were removed after 24 h. The cells were washed with phosphate buffered saline once and cell culture medium was added (150 µl/well). The cells were then allowed to grow for a further 72 h. The surviving cells were fixed by adding 150 µL/well of 50% (w/v) trichloroacetic acid and incubated for 1 h in a refrigerator (277 K). The plates were washed with tap water three times and dried under a flow of warm air, 0.4% sulforhodamine B (Sigma) solution (100 µL/well) was added, followed by washing with 1% acetic acid five times and drying under a flow of warm air. The dye was dissolved in 10 mM Tris buffer (200 µL/well). The absorbance of each well was determined using a Multiskan Ascent plate reader (Labsystems) at 540 nm. The absorbance of SRB in each well is directly proportional to the cell number. Then the

absorbance was plotted against concentration and the IC_{50} determined by using Origin software.

NAC (N-acetyl-L-cysteine) or L-BSO Combination Treatments. A2780 cells were treated with 50 μM NAC or L-BSO and various concentrations of osmium complexes for 24 h. Then NAC/L-BSO and osmium complexes were removed at the same time and cells washed with PBS once, then incubated for a further 72 h for recovery. Cell viability was determined using the SRB assay as described above.

Partition Coefficient (Log P) and Cellular uptake

Determination of log P. Octanol-saturated water and water-saturated octanol were prepared by stirring the mixture for 24 h. Aliquots of stock solutions of osmium complexes in octanol-saturated water (2 mL) were added to the same volumes of water-saturated octanol (2 mL) and shaken in an IKA Vibrax VXC basic shaker for 4 h at the speed of 500 g/min after partition. The aqueous layer was transferred into test tubes for osmium analysis. Aqueous samples before and after partitioning were diluted with 3.6 % HNO_3 to the appropriate range for analysis by ICP-MS calibrated with aqueous standards (osmium, 0.1-400 ppb). These procedures were carried out at ambient temperature (ca. 298 K). Log P values of osmium complexes were calculated using the equation $\log P_{oct} = \log([Os]_{oct}/[Os]_{aq})$.

.**ICP-MS Instrumentation and Calibration**. ICP-MS analyses were carried out on an Agilent Technologies 7500 series ICP-MS instrument. The water used for ICP-MS analysis was double deionized using a USF Elga UHQ PS water deionizer. The osmium Specpure plasma standard was diluted in double deionized water to 20 ppm. The osmium standards for calibration were freshly prepared by diluting this stock solution with 3.6 % HNO_3 in double deionized water. The concentrations used were 400, 200, 100, 50, 25, 10, 5, 1, 0.5 and 0.1 ppb.

Cellular uptake. A2780 cells were seeded 10^6 cells/well in 6-well plates. After 24 h incubation, cells were exposed to 4 μM osmium complex. After 1 h, 2 h, 4 h and 24 h of drug exposure, the drug-containing medium was removed. Then samples were

washed with PBS twice, trypsinized, collected and stored at 253 K until ICP-MS analysis for osmium content. The numbers of cells were counted using a cytometer. The whole cell pellets were digested as described below. Firstly, 0.5 mL of freshly distilled 72% HNO_3 was added to each 1 mL cells pellets, and the samples were transferred into Wheaton V-Vials The vials were heated in an oven at 373 K for 16 h to digest the samples fully, allowed to cool, and then transferred to Falcon tubes. The vials were washed with double deionized water three times and diluted 10 times with double deionized water to obtain 6% HNO_3 sample solutions. A blank and the standards were loaded into the sample tray and were run from the lowest to the highest concentration in a 'no gas' mode, followed by the samples.

Separation of Cell Fractions. The A2780 cells were seeded into Petri dishes at a concentration of $5*10^6$ cells/dish. After 24 h incubation, osmium compounds **9** (4 μM) and **23** (4 μM) were added. The cells were harvested after a further incubation with osmium compound for 24 h. Then the four cell fractions (cytosol, membrane plus particulate fraction, nucleus and cytoskeleton) were separated following the protocol described for the kit (BioVision, Inc, USA). The concentrations of osmium in different fractions were measured by ICP-MS after digestion following the same method as for the cellular uptake study.

Detection of ROS. The vial of DCFH-DA was opened under N_2 protection, and contents dissolved in DMSO to give a 10 mM stock solution . A2780 cells were seeded (5000 cells/well) into black 96-well plates and incubated for 24 h at 310 K, 5% CO_2, high humidity. Cells were loaded with DCFH-DA (10 μM) and incubated for 30 min. The probe was removed and PBS was used to wash the cells twice. The cells were then kept in PBS solution and osmium compound **9** (4 μM), or NAC (50 μM) with **9** (4 μM)**,** or L-BSO (50 μM) with **9** (4 μM) were added. Hydrogen peroxide (50 μM) was added as the positive control. The fluorescence was recorded over a period of 4 h at 310 K by excitation at 480 nm and emission at 530 nm on a TECAN plate reader.

Acknowledgements. We thank Dr. Michael Khan (Life Sciences) and Dr Ana Pizarro (Chemistry) for provision of facilities for cell culture, Professor. Tim Bugg for use of a microplate reader, Dr Lijiang Song and Mr Philip R. Aston for assistance with ICP-MS and the ERC (247450 BIOINCMED), EPSRC and Science City/EU ERDF/AWM for funding.

Notes and references:

1. B. Rosenberg, L. Vancamp, J. E. Trosko and V. H. Mansour, *Nature*, 1969, **222**, 385-386.
2. C. G. Hartinger and P. J. Dyson, *Chem. Soc. Rev.*, 2009, **38**, 391-401.
3. G. Gasser, I. Ott and N. Metzler-Nolte, *J. Med. Chem.*, 2010, **54**, 3-25.
4. H. Elizabeth, V. Anne, T. Laurent, J. Gérard and A. Christian, *Angew. Chem., Int. Ed.*, 2006, **118**, 291-296.
5. R. E. Morris, R. E. Aird, P. del Socorro Murdoch, H. Chen, J. Cummings, N. D. Hughes, S. Parsons, A. Parkin, G. Boyd, D. I. Jodrell and P. J. Sadler, *J. Med. Chem.*, 2001, **44**, 3616-3621.
6. R. E. Aird, J. Cummings, A. A. Ritchie, M. Muir, R. E. Morris, H. Chen, P. J. Sadler and D. I. Jodrell, *Br. J. Cancer.*, 2002, **86**, 1652-1657.
7. C. Scolaro, A. Bergamo, L. Brescacin, R. Delfino, M. Cocchietto, G. Laurenczy, T. J. Geldbach, G. Sava and P. J. Dyson, *J. Med. Chem.*, 2005, **48**, 4161-4171.
8. H. Chen, J. A. Parkinson, S. Parsons, R. A. Coxall, R. O. Gould and P. J. Sadler, *J. Am. Chem. Soc.*, 2002, **124**, 3064-3082.
9. K. V. Kong, W. K. Leong and L. H. K. Lim, *Chem. Res. Toxicol.*, 2009, **22**, 1116-1122.
10. L. K. Filak, G. Mühlgassner, F. Bacher, A. Roller, M. Galanski, M. A. Jakupec, B. K. Keppler and V. B. Arion, *Organometallics*, 2010, **30**, 273-283.
11. M. Hanif, A. A. Nazarov, C. G. Hartinger, W. Kandioller, M. A. Jakupec, V. B. Arion, P. J. Dyson and B. K. Keppler, *Dalton Trans.*, 2010, **39**, 7345-7352.
12. W.-X. Ni, W.-L. Man, M. T.-W. Cheung, R. W.-Y. Sun, Y.-L. Shu, Y.-W. Lam, C.-M. Che and T.-C. Lau, *Chem. Commun.*, 2011, **47**, 2140-2142.
13. F. A. P. Anna and J. S. Peter, *Chem.- Asian. J.*, 2008, **3**, 1890-1899.
14. A. Bergamo, A. Masi, A. F. A. Peacock, A. Habtemariam, P. J. Sadler and G. Sava, *J. Inorg. Biochem.*, **104**, 79-86.
15. K. Kien Voon, L. Weng Kee, N. Swee Phyaw, N. Thanh Hung and H. K. L. Lina, *ChemMedChem*, 2008, **3**, 1269-1275.
16. A. Dorcier, W. H. Ang, S. BolaÃ±o, L. Gonsalvi, L. Juillerat-Jeannerat, GÃ b. Laurenczy, M. Peruzzini, A. D. Phillips, F. Zanobini and P. J. Dyson, *Organometallics*, 2006, **25**, 4090-4096.
17. A. F. A. Peacock, S. Parsons and P. J. Sadler, *J. Am. Chem. Soc.*, 2007, **129**, 3348-3357.
18. M. Jasna, S. W. Douglas , G. E. Atilla-Gokcumen, S. M. S. Keiran , J. C. Patrick , D. W. Richard , F. Panagis, K. Stefan, H. Meenhard and M. Eric, *Chem.-Eur. J.*, 2008, **14**, 4816-4822.
19. B. Cebrián-Losantos, A. A. Krokhin, I. N. Stepanenko, R. Eichinger, M. A. Jakupec, V. B. Arion and B. K. Keppler, *Inorg. Chem.*, 2007, **46**, 5023-5033.
20. D. J. Ward, H. Sheppeard, *Rheumatol. Rehabil.*, 1980, **19**, 25-29.
21. F. E. Berglof, *Acta. Rheumatol. Scand.*, 1959, **5**, 70-74.
22. C. J. Menkes, *Rheumatology*, 1979, **18**, 65-77.
23. *Platinum, Gold, and Other Metal Chemotherapeutic Agents*, ed. C. Hinckley C, N. Bemiller J, E. Strack L and D. Russell L, Ameican Chemical Society, 1983.

24. Y. Fu, A. Habtemariam, A. M. Pizarro, S. H. van Rijt, D. J. Healey, P. A. Cooper, S. D. Shnyder, G. J. Clarkson and P. J. Sadler, *J. Med. Chem.*, 2010, **53**, 8192-8196.
25. S. D. Shnyder, Y, Fu, A. Habtemariam,S. H. van Rijt, P. A. Cooper, P. M. Loadman, P. J. Sadler, *MedChemComm*, 2011, *DOI:10.1039/C1MD00*
26. S. J. Dougan, A. Habtemariam, S. E. McHale, S. Parsons and P. J. Sadler, *Proc. Natl. Acad. Sci. U. S. A.*, 2008, **105**, 11628-11633.
27. S. H. van Rijt, A. Mukherjee, A. M. Pizarro and P. J. Sadler, *J. Med. Chem.*, 2009, **53**, 840-849.
28. D. F. Veber, S. R. Johnson, H.-Y. Cheng, B. R. Smith, K. W. Ward and K. D. Kopple, *J. Med. Chem.*, 2002, **45**, 2615-2623.
29. Y. C. Martin, *J. Med. Chem.*, 1981, **24**, 229-237.
30. K. Birchall, V. J. Gillet, P. Willett, P. Ducrot and C. Luttmann, *J. Chem. Inf. Model*., 2009, **49**, 1330-1346.
31. G. A. Patani and E. J. LaVoie, *Chem. Rev.*, 1996, **96**, 3147-3176.
32. J. E. Liebmann, S. M. Hahn, J. A. Cook, C. Lipschultz, J. B. Mitchell and D. C. Kaufman, *Cancer. Res.*, 1993, **53**, 2066-2070.
33. S. H. van Rijt, A. J. Hebden, T. Amaresekera, R. J. Deeth, G. J. Clarkson, S. Parsons, P. C. McGowan and P. J. Sadler, *J. Med. Chem.*, 2009, **52**, 7753-7764.
34. M. J. McKeage, S. J. Berners-Price, P. Galettis, R. J. Bowen, W. Brouwer, L. Ding, L. Zhuang and B. C. Baguley, *Cancer. Chemother. Pharmacol.*, 2000, **46**, 343-350.
35. B. Halliwell and M. Whiteman, *Br. J. Pharmacol.*,2004, **142**, 231-255.
36. H. Wang and J. A. Joseph, *Free. Radic. Biol. Med*., 1999, **27**, 612-616.
37. A. Gomes, E. Fernandes and J. L. F. C. Lima, *J. Biochem. Biophys. Methods.*, 2005, **65**, 45-80.
38. R. F. Ozols, K. G. Louie, J. Plowman, B. C. Behrens, R. L. Fine, D. Dykes and T. C. Hamilton, *Biochem. Pharmacol.*, 1987, **36**, 147-153.
39. O. I. Aruoma, B. Halliwell, B. M. Hoey and J. Butler, *Free. Radic. Biol. Med*., 1989, **6**, 593-597.
40. S. J. Dougan, M. Melchart, A. Habtemariam, S. Parsons and P. J. Sadler, *Inorg. Chem.*, 2006, **45**, 10882-10894.
41. C. A. Hunter and J. K. M. Sanders, *J. Am. Chem. Soc*., 1990, **112**, 5525-5534.
42. O. Novakova, H. Chen, O. Vrana, A. Rodger, P. J. Sadler and V. Brabec, *Biochemistry*, 2003, **42**, 11544-11554.
43. W. Hu, Q. Luo, X. Ma, K. Wu, J. Liu, Y. Chen, S. Xiong, J. Wang, P. J. Sadler and F. Wang, *Chem.-Eur. J*., 2009, **15**, 6586-6594.
44. D. Trachootham, J. Alexandre and P. Huang, *Nat. Rev. Drug. Discov.*, 2009, **8**, 579-591.
45. L. K. Hosking, R. D. H. Whelan, S. A. Shellard, P. Bedford and B. T. Hill, *Biochem. Pharmacol*.,1990, **40**, 1833-1842.
46. Z. H. Siddik, *Oncogene*, **22**, 7265-7279.
47. H. H. Bailey, R. T. Mulcahy, K. D. Tutsch, R. Z. Arzoomanian, D. Alberti, M. B. Tombes, G. Wilding, M. Pomplun and D. R. Spriggs, *J. Clin. Oncol.*, 1994, **12**, 194-205.
48. T. C. Hamilton, M. A. Winker, K. G. Louie, G. Batist, B. C. Behrens, T. Tsuruo, K. R. Grotzinger, W. M. McKoy, R. C. Young and R. F. Ozols, *Biochem. Pharmacol*., 1985, **34**, 2583-2586.

49. H. Maeda, S. Hori, H. Ohizumi, T. Segawa, Y. Kakehi, O. Ogawa and A. Kakizuka, *Cell Death Differ*., 2004, **11**, 737-746.
50. E. A. Meyer, R. K. Castellano and F. Diederich, *Angew. Chem., Int. Ed*.,2003, **42**, 1210-1250.
51. J. A. Platts, D. E. Hibbs, T. W. Hambley and M. D. Hall, *J. Med. Chem.*, 2000, **44**, 472-474.
52. M. Groessl, E. Reisner, C. G. Hartinger, R. Eichinger, O. Semenova, A. R. Timerbaev, M. A. Jakupec, V. B. Arion and B. K. Keppler, *J. Med. Chem.*, 2007, **50**, 2185-2193.
53. F. Yu, J. Megyesi and P. M. Price, *Am. J. Physiol. Renal Physiol.*, 2008, **295**, F44-52.
54. E. R. Jamieson and S. J. Lippard, *Chem. Reviews.*, 1999, **99**, 2467-2498.
55. A. F. A. Peacock, A. Habtemariam, S. A. Moggach, A. Prescimone, S. Parsons and P. J. Sadler, *Inorg. Chem.*, 2007, **46**, 4049-4059.
56. O*xford Diffraction: Wroclaw, Poland*, 2007, **171**, 5.
57. G. M. Sheldrick, *Acta Cryst*, 1990, **A46**, 467-473.
58. G. M. Sheldrick, *SHELX97*, 1997, Programs for Crystal Structure Analysis (Release 97-92); University of Göttingen, Germany.
59. V. Vichai and K. Kirtikara, *Nat. Protocols*, 2006, **1**, 1112-1116.

Chart 1. Osmium phenylazopyridine arene complexes studied in this work.

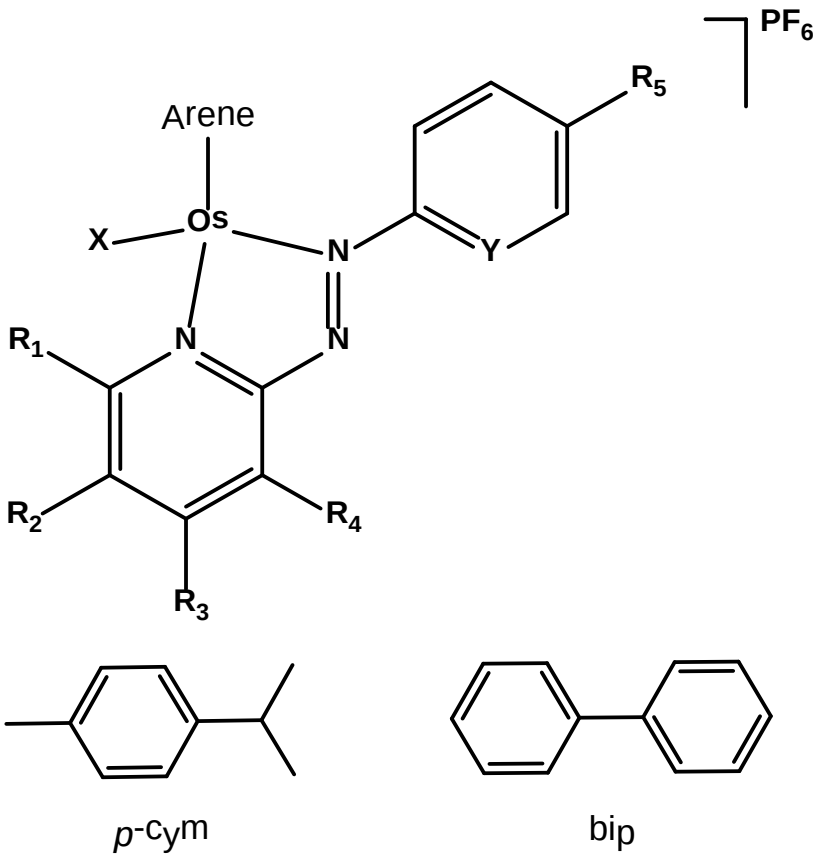

p-cym

bip

Complex	Arene	R_1	R_2	R_3	R_4	R_5	X	Y
1	bip	CF_3	H	H	Cl	H	I	C
2	*p*-cym	CF_3	H	H	Cl	H	I	C
3	bip	CF_3	H	H	Cl	H	Cl	C
4	*p*-cym	CF_3	H	H	Cl	H	Cl	C
5	bip	Cl	H	H	H	H	I	C
6	*p*-cym	Cl	H	H	H	H	I	C
7*	bip	Cl	H	H	H	H	Cl	C
8	*p*-cym	Cl	H	H	H	H	Cl	C
9	bip	H	F	H	H	H	I	C
10*	bip	H	F	H	H	H	Cl	C
11	*p*-cym	H	F	H	H	H	I	C
12	*p*-cym	H	F	H	H	H	Cl	C
13*	bip	H	Cl	H	H	H	I	C
14*	*p*-cym	H	Cl	H	H	H	I	C
15	bip	H	Cl	H	H	H	Cl	C
16*	*p*-cym	H	Cl	H	H	H	Cl	C
17	bip	H	Br	H	H	H	I	C
18*	*p*-cym	H	Br	H	H	H	I	C
19*	bip	H	Br	H	H	H	Cl	C
20*	*p*-cym	H	Br	H	H	H	Cl	C
21	bip	H	I	H	H	H	I	C
22	*p*-cym	H	I	H	H	H	I	C
23	bip	H	H	Cl	H	H	I	C
24*	*p*-cym	H	H	Cl	H	H	I	C
25	bip	H	H	Cl	H	H	Cl	C
26*	*p*-cym	H	H	Cl	H	H	Cl	C
27	bip	H	H	H	H	H	I	N
28	*p*-cym	H	H	H	H	H	I	N
29	bip	H	H	H	H	H	Cl	N
30	*p*-cym	H	H	H	H	H	Cl	N
31	*p*-cym	H	H	OH	H	NO_2	I	C
32	*p*-cym	H	H	OH	H	NO_2	Cl	C

* X-ray structure determined

Table 1. (A) IC_{50} values for A2780 cells for complexes **1**-**32**. **(B)** Comparison of IC_{50} values for A2780 cells for monodentate ligand = Cl or I. **(C)** Comparison of IC_{50} values for A2780 cells for arene - *p*-cym or bip.

(A)

Complex	IC_{50} (μM)
(**1**) [Os(η^6-bip)(1-CF_3-4-Cl-Azpy)I]PF_6	5.7(±1.0)
(**2**) [Os(η^6-*p*-cym)(1-CF_3-4-Cl-Azpy)I]PF_6	10.9(±0.3)
(**3**) [Os(η^6-bip)(1-CF_3-4-Cl-Azpy)Cl]PF_6	25.2(±0.1)
(**4**) [Os(η^6-*p*-cym)(1-CF_3-4-Cl-Azpy)Cl]PF_6	38.2(±2.8)
(**5**) [Os(η^6-bip)(1-Cl-Azpy)I]PF_6	3.7(±0.3)
(**6**) [Os(η^6-*p*-cym)(1-Cl-Azpy)I]PF_6	9.0(±4.5)
(**7**) [Os(η^6-bip)(1-Cl-Azpy)Cl]PF_6	42.9(±5.4)
(**8**) [Os(η^6-*p*-cym)(1-Cl-Azpy)Cl]PF_6	24.0(±0.1)
(**9**) [Os(η^6-bip)(2-F-Azpy)I]PF_6	0.63(±0.1)
(**10**) [Os(η^6-bip)(2-F-Azpy)Cl]PF_6	>100
(**11**) [Os(η^6-*p*-cym)(2-F-Azpy)I]PF_6	6.0(±0.4)
(**12**) [Os(η^6-*p*-cym)(2-F-Azpy)Cl]PF_6	13.3(±0.7)
(**13**) [Os(η^6-bip)(2-Cl-Azpy)I]PF_6	1.0(±0.1)
(**14**) [Os(η^6-*p*-cym)(2-Cl-Azpy)I]PF_6	33.6(±2.0)
(**15**) [Os(η^6-bip)(2-Cl-Azpy)Cl]PF_6	>50
(**16**) [Os(η^6-*p*-cym)(2-Cl-Azpy)Cl]PF_6	30.2(±12.4)
(**17**) [Os(η^6-bip)(2-Br-Azpy)I]PF_6	0.59(±0.02)
(**18**) [Os(η^6-*p*-cym)(2-Br-Azpy)I]PF_6	36.6(±0.9)
(**19**) [Os(η^6-bip)(2-Br-Azpy)Cl]PF_6	>50
(**20**) [Os(η^6-*p*-cym)(2-Br-Azpy)Cl]PF_6	>50
(**21**) [Os(η^6-bip)(2-I-Azpy)I]PF_6	0.22(±0.02)
(**22**) [Os(η^6-*p*-cym)(2-I-Azpy)I]PF_6	2.4(±0.5)
(**23**) [Os(η^6-bip)(3-Cl-Azpy)I]PF_6	22.0(±2.0)
(**24**) [Os(η^6-*p*-cym)(3-Cl-Azpy)I]PF_6	48.4(±6.1)
(**25**) [Os(η^6-bip)(3-Cl-Azpy)Cl]PF_6	>100
(**26**) [Os(η^6-*p*-cym)(3-Cl-Azpy)Cl]PF_6	>100
(**27**) [Os(η^6-bip)(Abpy))I]PF_6	21.3(±6.2)
(**28**) [Os(η^6-*p*-cym)(Abpy))I]PF_6	10.8(±0.11)
(**29**) [Os(η^6-bip)(Abpy)Cl]PF_6	22.4(±11.8)
(**30**) [Os(η^6-*p*-cym)(Abpy))Cl]PF_6	>100
(**31**) [Os(η^6- *p*-cym)(OH-Azpy-NO_2)I]PF_6	0.29(±0.04)
(**32**) [Os(η^6-*p*-cym)(OH-Azpy-NO_2)Cl]PF_6	0.30(±0.05)

(B)

Cl complex / I complex	**IC_{50} (Cl) / IC_{50} (I)**
3/1	4.4
4/2	3.5
7/5	11.6
8/6	2.7
10/9	>159
12/11	2.2
15/13	>50
16/14	0.9
19/17	>85
20/18	>1.4
25/23	>4.5
26/24	>2.1
29/27	1.0

(C)

***p*-Cym Complex / Bip Complex**	**IC_{50} (*p*-Cym) / IC_{50} (Bip)**
2/1	1.91
4/3	1.52
6/5	2.43
8/7	0.56
12/10	>7.5
14/13	33.6
18/17	62.0
22/21	10.9
24/23	2.20
28/27	0.51

Table 2. IC_{50} values of combination treatment with NAC or L-BSO. **(A)** Effect of L-BSO treatment (24 h) on IC_{50} values for A549 human lung cancer cells. **(B)** Effect of L-BSO and NAC treatment (24 h) on IC_{50} values for IC_{50} values for A2780 human ovarian cancer cells. The error bars are standard deviations from an average of three wells.

(A)

Complex	IC_{50}/μM	+ L-BSO IC_{50} /μM
9	1.8 (±1.4)	>100
17	3.6 (±0.2)	30.5 (±2.6)

(B)

Complex	IC_{50}/μM	+ L-NAC IC_{50} /μM	+ L-BSO IC_{50} /μM
9	0.63 (±0.10)	0.97 (±0.00)	12.6 (±1.9)
17	0.59 (±0.02)	1.14 (±0.22)	8.4 (±0.9)

Figure captions

Fig 1. X-ray crystal structures of the cations of [Os(η^6-bip)(1-Cl-Azpy)Cl]PF_6 (**7**) [Os(η^6-bip)(2-F-Azpy)Cl]PF_6 (**10**), [Os(η^6-bip)(2-Cl-Azpy)I]PF_6 (**13**), [Os(η^6-*p*-cym)(2-Cl-Azpy)I]PF_6 (**14**), [Os(η^6-*p*-cym)(2-Cl-Azpy)Cl]PF_6 (**16**), [Os(η^6-*p*-cym)(2-Br-Azpy)I]PF_6 (**18**), [Os(η^6-bip)(2-Br-Azpy)Cl]PF_6 (**19**), [Os(η^6-*p*-cym)(2-Br-Azpy)Cl]PF_6 (**20**), [Os(η^6-*p*-cym)(3-Cl-Azpy)I]PF_6 (**24**) and [Os(η^6-*p*-cym)(3-Cl-Azpy)Cl]PF_6 (**26**) with thermal ellipsoids drawn at 50% probability. The hydrogen atoms, counterions (PF_6) and solvent water molecules have been omitted for clarity

Fig 2. Comparision of the effect of different pyridine ring substitutions on IC_{50} values for A2780 cells. Different colours were employed to show different sub-family of these complexes: green (arene = biphenyl, monodentate ligand=iodide), orange (arene = biphenyl, monodentate ligand = chloride), blue (arene = *para*-cymene, monodentate ligand = iodide), red (arene = *para*-cymene, monodentate ligand = chloride). **(A)** Chloride substituent at R_1, R_2 and R_3 positions. **(B)** Fluoride, chloride, bromide or iodide substituent at R_2 position.

Fig 3. Comparison of octanol/water partition coefficients (log P values) and cytotoxicity towards A2780 cells.

Fig 4. Uptake of osmium into A2780 human ovarian cancer cells. **(A)** Time dependence for complexes **9** and **23 (B)** Osmium distribution of Os from complexes **9** and **23** in cell fractions: cytosol, membrane plus particulate fraction, nucleus and cytoskeleton. Data are the mean of three experiments and are reported as mean ± standard error of the mean (SEM)

Fig 5. (**A**) Relative changes in DCF fluorescence detected over time after exposure to 1 μM **9**, 1 μM **9** with 50 μM NAC, 1 μM **9** with 50 μM L-BSO, or 50 μM H_2O_2. For

each compound, the fluorescence was averaged over 6 wells (n = 6). (**B**) Percentage cell survival after 24 h exposure to 50 μM NAC (C+NAC), 50 μM L-BSO (C+L-BSO), 1 μM **9** (9), 1 μM **9** with 50 μM NAC (9+NAC), 1 μM **9** with 50 μM L-BSO (9+ L-BSO) and 96 h recovery for A2780 ovarian cancer cells; effects of combination treatment of complex [Os(η^6-bip)(2-F-Azpy)I]PF_6 (**9)** or [Os(η^6-bip)(2-Br-Azpy)I]PF_6 (**17**) with NAC or L-BSO.

Fig 1.

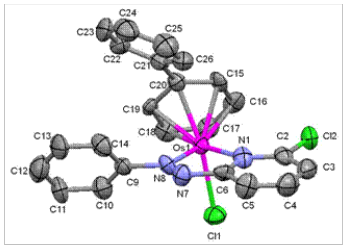

(7)

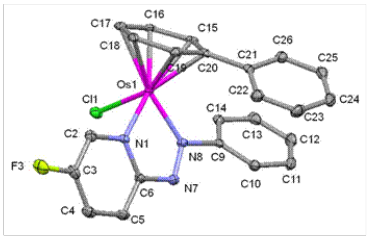

(10)

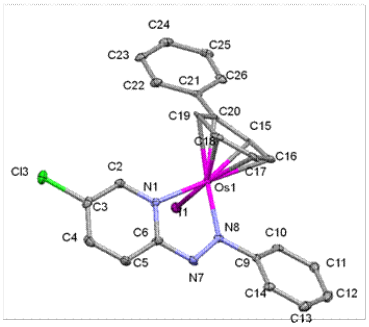

(13)

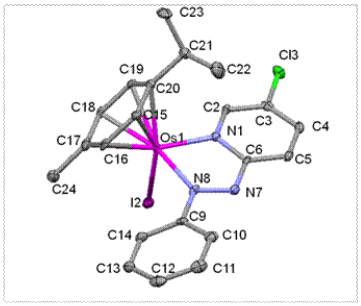

(14)

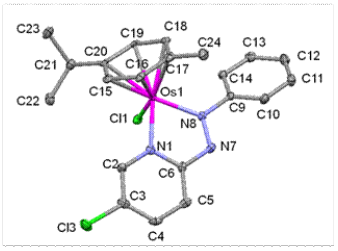

(16)

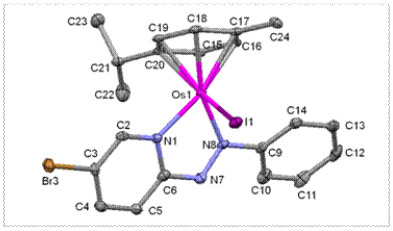

(18)

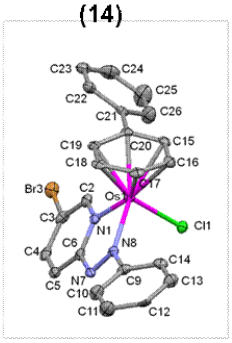

(19)

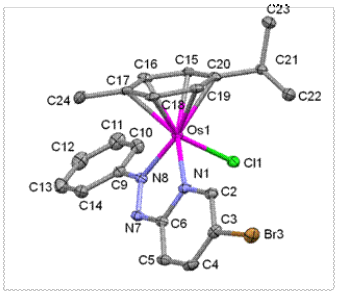

(20)

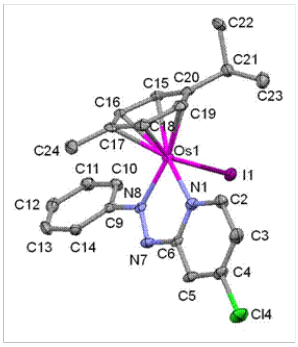

(24)

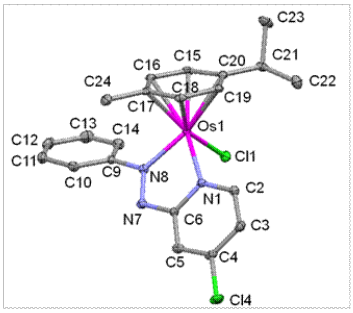

(26)

Fig. 2

(A)

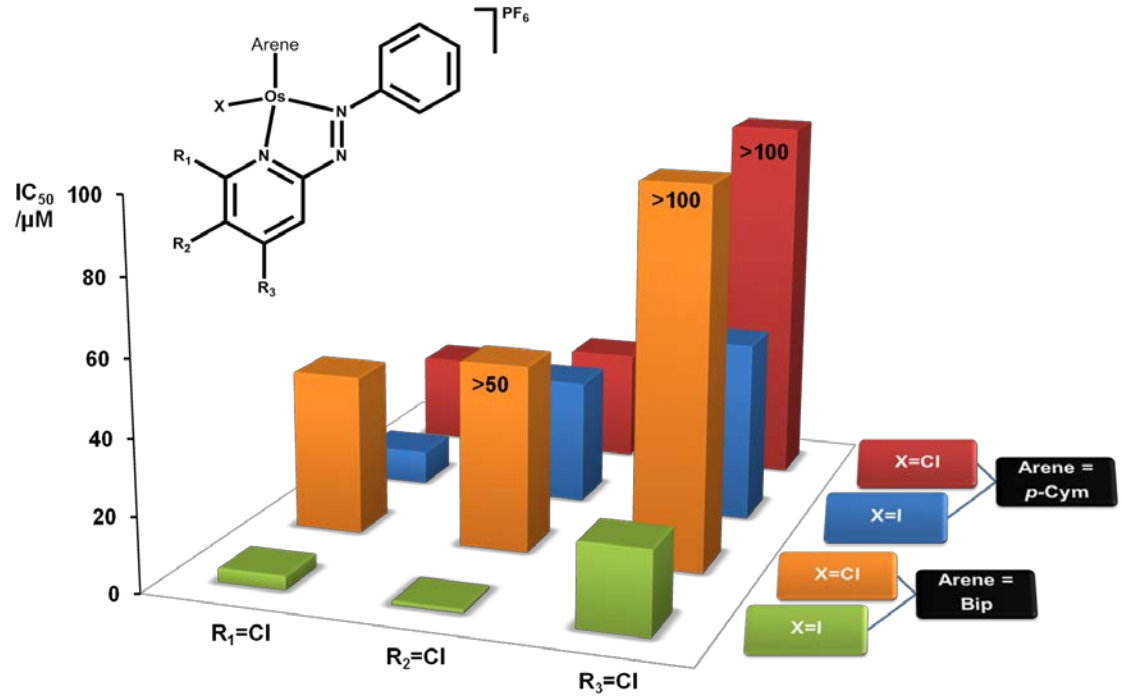
Arene
X
Os
N
N
N
N
R1
R2
R3
PF6
IC50 /μM
100
80
60
40
20
0
>100
>100
>50
R1=Cl
R2=Cl
R3=Cl
X=Cl
X=I
Arene = p-Cym
X=Cl
X=I
Arene = Bip

(B)

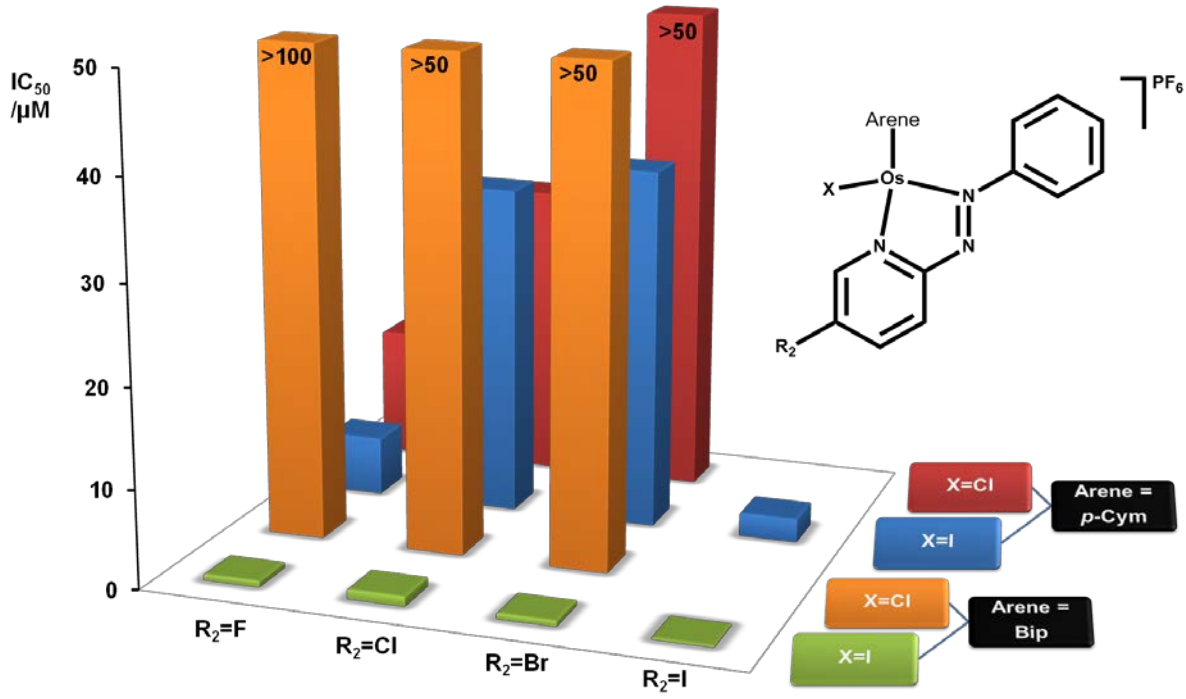
IC50 /μM
50
40
30
20
10
0
>100
>50
>50
>50
R2=F
R2=Cl
R2=Br
R2=I
Arene
X
Os
N
N
N
N
R2
PF6
X=Cl
X=I
Arene = p-Cym
X=Cl
X=I
Arene = Bip

Fig. 3

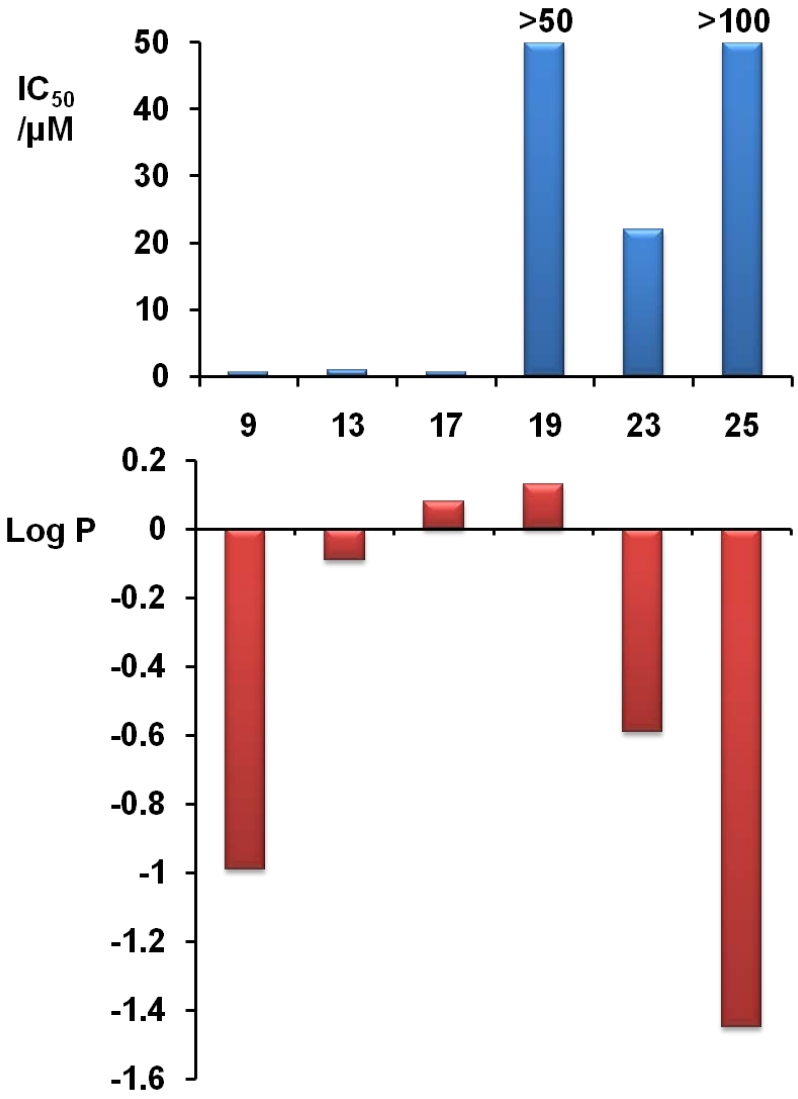
IC50 /μM
50
40
30
20
10
0
>50
>100
9
13
17
19
23
25
Log P
0.2
0
-0.2
-0.4
-0.6
-0.8
-1
-1.2
-1.4
-1.6

Fig 4.

(A)

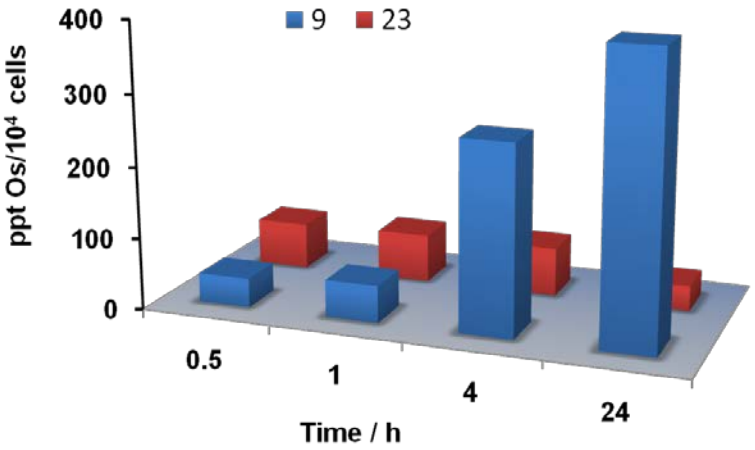
9
23
400
300
200
100
0
ppt Os/10⁴ cells
0.5
1
4
24
Time / h

(B)

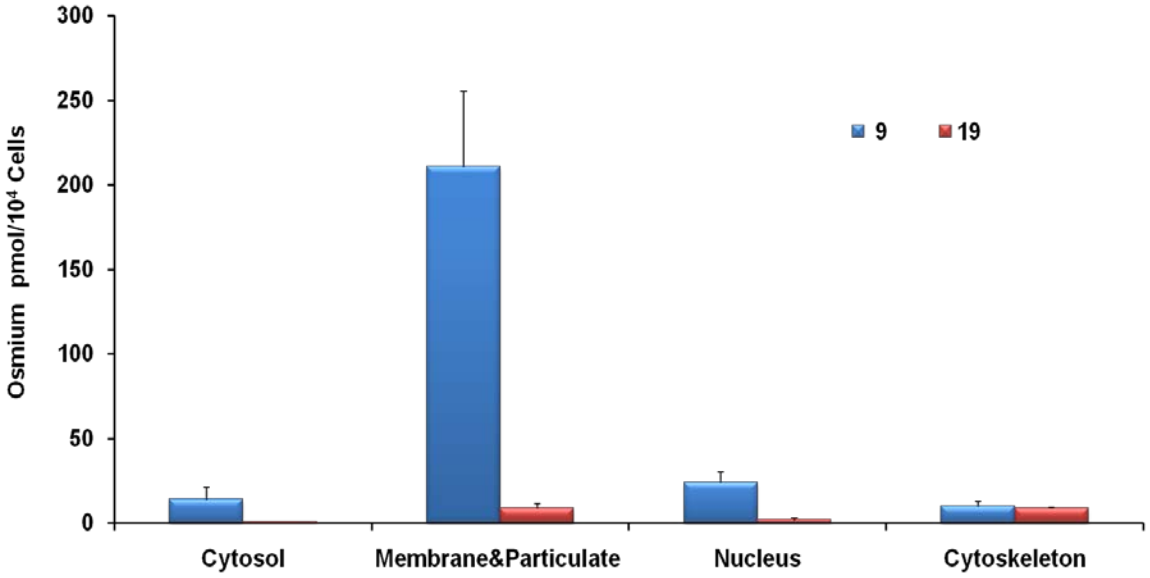
300
250
200
150
100
50
0
Osmium pmol/10⁴ Cells
9
19
Cytosol
Membrane&Particulate
Nucleus
Cytoskeleton

Fig. 5

(A)

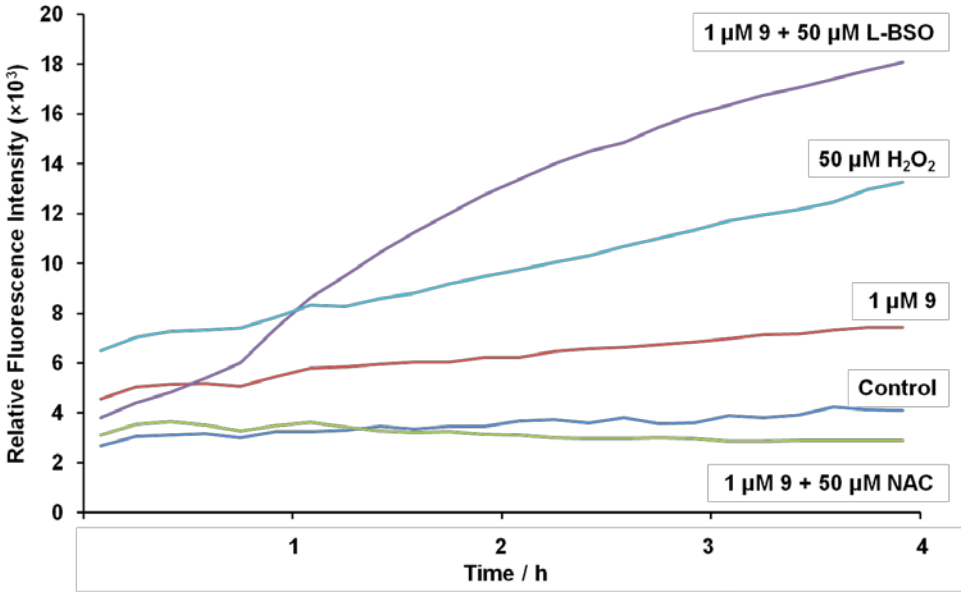
Relative Fluorescence Intensity (×10³)
Time / h
1 μM 9 + 50 μM L-BSO
50 μM H2O2
1 μM 9
Control
1 μM 9 + 50 μM NAC

(B)

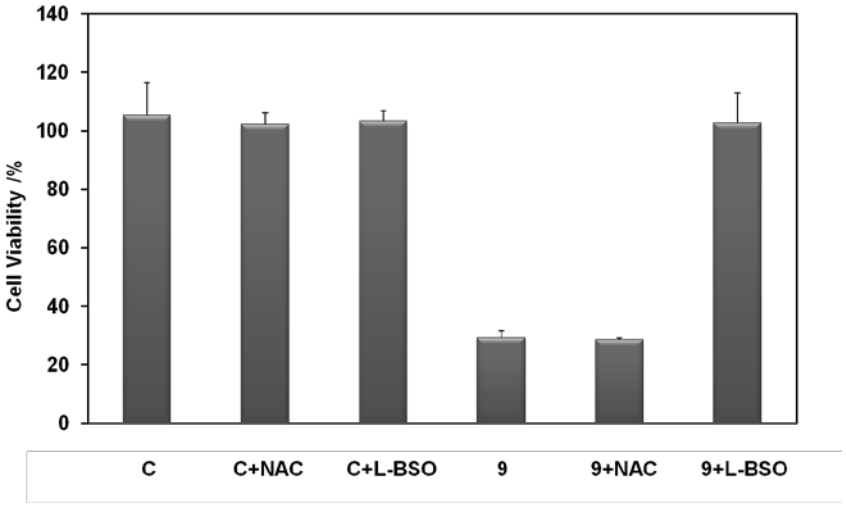
Cell Viability /%
C
C+NAC
C+L-BSO
9
9+NAC
9+L-BSO